Journal of the Neurological Sciences 398 (2019) 148–156

Contents lists available at ScienceDirect

Journal of the Neurological Sciences

journal homepage: www.elsevier.com/locate/jns

A retrospective evaluation of thalamic targeting for tremor deep brain stimulation using high-resolution anatomical imaging with supplementary fiber tractography

Takashi Morishita[a,*], Masa-aki Higuchi[b], Hiromasa Kobayashi[a], Hiroshi Abe[a], Toshio Higashi[a], Tooru Inoue[a]

[a] Department of Neurosurgery, Fukuoka University, Faculty of Medicine, Fukuoka, Japan
[b] Department of Neurology, Higuchi Hospital, Saga, Japan

ARTICLE INFO

Keywords:
Diffusion tensor image
Fiber tractography
Tremor
Deep brain stimulation
Fast gray matter acquisition T1 inversion recovery

ABSTRACT

Objectives: Deep brain stimulation (DBS) of the ventral intermediate (Vim) thalamic nucleus is used to treat tremors. Here, we identified the Vim nucleus on fast gray matter acquisition T1 inversion recovery (FGATIR) images and delineated the dentate-rubrothalamic tract (DRT) to determine the DBS target. We evaluated whether this method could consistently identify the Vim nucleus by anatomical imaging and fiber tractography.

Methods: We retrospectively reviewed clinical data of patients who underwent unilateral thalamic DBS for severe tremor disorders. We evaluated outcomes at baseline, 6 months and 1 year following intervention, and annually thereafter. We reviewed preoperative planning to determine whether our tractography technique could consistently depict the DRT, and evaluated implanted electrode position by fusing postoperative CT scans to preoperative MR images.

Results: Seven patients (three men and four women) were included; preoperative diagnoses included essential tremor (n = 3), Parkinson's (n = 2), and Holmes tremor (n = 2). All patients responded to DBS therapy; motor scores improved at 6-month and last follow-up. The Vim nucleus was successfully identified, as the DRT was depicted in all cases. Of ten active DBS contacts in seven leads, four contacts were located outside of the depicted DRT, and these contacts tended to require higher stimulation intensity.

Conclusions: The Vim nucleus was successfully identified with FGATIR. Our methods may be useful to determine optimal DBS trajectory, and potentially improve outcomes.

1. Introduction

Deep brain stimulation (DBS[1]) has proven to be an effective treatment option for tremor disorders; such surgical interventions target thalamic nuclei, including the ventral intermediate (Vim) and the ventralis oralis (Vo) nuclei. Recent advances in the quality of neuroimaging have improved the accuracy and safety of DBS surgery; several groups have reported the application of diffusion tensor imaging (DTI) and fiber tractography paired with magnetic resonance imaging (MRI) for stereotactic planning [1–5]. However, most institutions that perform thalamic DBS surgery to treat tremor disorders employ the classic indirect targeting technique; the target is identified based on neuroanatomical landmarks such as the width of the third ventricle and the distance between the anterior commissure (AC) and the posterior commissure (PC) [6,7]. Irrespective of targeting strategy, finding an accurate target for intervention remains difficult.

To address the problem of visualizing the thalamic nuclei, several studies have reported unique in-house techniques; these include a deformable 3D brain atlas [8,9] and fiber tractography of the dentate-rubrothalamic tract (DRT) connecting the dentate nucleus in the cerebellum and the contralateral Ventrolateral nucleus including Vo and Vim nuclei [3,4,10–12]. While the former techniques are useful in

* Corresponding author at: Department of Neurosurgery, Fukuoka University Faculty of Medicine, Nanakuma 7-45-1, Jonan ward, Fukuoka 814-0180, Japan.
E-mail address: tmorishita@fukuoka-u.ac.jp (T. Morishita).

[1] Deep brain stimulation, DBS; ventral intermediate, Vim; ventralis oralis, Vo; diffusion tensor imaging, DTI; magnetic resonance imaging, MRI; anterior commissure, AC; posterior commissure, PC; dentate-rubrothalamic tract, DRT; red nucleus, RN; fast gray matter acquisition T1 inversion recovery, FGATIR; region of interest, ROI; tremor rating scale, TRS; computed tomography, CT; T1-weighted imaging, T1WI; mid-commissural, MC; caudal zona incerta, cZi; microelectrode recording, MER; implantable pulse generator, IPG; postoperative day, POD; Parkinson's disease, PD; essential tremor, ET; mammillothalamic tract, MTT; centromedian, CM; mediodorsal, MD; parafacicullar, Pf.

https://doi.org/10.1016/j.jns.2019.01.025
Received 3 August 2018; Received in revised form 22 December 2018; Accepted 15 January 2019
Available online 16 January 2019
0022-510X/

identifying the thalamic nuclei, it is usually difficult to match the atlas to an individual brain due to the commercialized software's lack of flexibility when atlas morphing. Conversely, fiber tractography has proven useful when stimulating the subthalamic area, but a standardized technique to visualize the fiber has yet to be developed [13].

In our practice, we have identified the Vim nucleus on fast gray matter acquisition T1 inversion recovery (FGATIR) images and have delineated the DRT determine the DBS target in tremor cases. We herein hypothesized that by depicting the DRT via high-resolution MRI and selecting the presumed Vim thalamic nucleus as a region of interest (ROI), the Vim nucleus may be consistently identified, thus improving clinical outcomes. This study further aimed to evaluate our unique DBS technique using high-resolution anatomical imaging with supplementary fiber tractography.

2. Material and methods

2.1. Study design

We retrospectively reviewed the clinical data of patients who underwent unilateral thalamic DBS for severe tremor disorders at our institution between January 2015 and September 2017. The diagnoses were made by movement disorder neurologists, and medically refractory tremor cases were indicated for DBS surgery; performed with written informed consent, the intervention was conducted unilaterally to treat the more severe side. Using the tremor rating scale (TRS), clinical evaluations were performed at baseline, as well as at the following time points following surgery: 6 months, 1 year, and annually thereafter. We only included patients who completed at least the six-month follow-up in this study. A Wilcoxon signed-rank test was performed to compare the follow-up TRS scores with the baseline condition. We also evaluated the position of the implanted electrode by means of a postoperative computed tomography (CT) scan fused with the preoperative MR image. This study was conducted with the approval of our institutional review board (IRB) named Fukuoka University-Medical Ethics Review Board (IRB approval number: 2017 M131) and was carried out in accordance with the Code of Ethics of the World Medical Association.

2.2. Stereotactic planning

An MRI scan was performed a few days prior to surgery using an MRI scanner (Ingenia 1.5 T, Philips, Netherland). Our MRI protocol for DBS planning included high-resolution volumetric T1-weighted imaging (T1WI) with contrast, FGATIR [8], and DTI imaging. The following parameters were applied for FGATIR: slice thickness, 1.5 mm; 240 slices; field of view, 240 × 240 × 180 mm^3; matrix size, 240 × 237 (0.75 mm^3 resolution); repetition/inversion/echo time, 3000/1500/4.29 ms; flip angle, 4 u; and bandwidth, 140 Hz/pixel. Image acquisition parameters for DTI imaging were as follows: slice thickness, 2.5 mm; 55 slices; field of view, 230 × 230 × 137.5 mm^3; matrix size, 92 × 90 (2.5 mm^3 resolution); TR 3472 ms; TE 89 ms; and b value, 800 s/mm^2.

Anatomical 3D image construction and stereotactic planning were performed using commercialized software (iPlan stereotaxy, Brainlab, Germany) prior to surgery. Multiple MRI sequences were automatically fused by the software. Following the image fusion process, we identified the AC, PC, and a midline plane to anchor the Cartesian coordinate system. The tentative target point was set at 11 mm lateral to the midline plane, 7 mm posterior to mid-commissural (MC) point, and 2 mm inferior to AC-PC line; the tip of the electrode could thus be placed in the caudal zona incerta (cZi).

To refine the trajectory, the parcellation of the ventrolateral thalamic nuclei on the FGATIR image were interpreted according to Hassler's classification by comparing the image against a human brain atlas (Fig. 1) [14]. The tentative trajectory was then modified based on the anatomical variation of each case so that the final trajectory of the DBS lead would pass through the Vo/Vim border and avoid blood vessels, sulci, and ventricles to ensure safety; this was performed by similar means to those reported by Foote and Okun [15]. As the interpretation of the thalamic parcellation on the FGATIR images has not been thoroughly discussed previously, we tested our interpretation by depicting the fiber tractography passing through both of the Vim nucleus and the RN.

As a part of stereotactic planning, the fiber tractography of the DRT was depicted using the “fiber tracking” function of the planning software. This function applies the deterministic tractography algorism with ROI approach to enable 3D reconstruction of the fiber tract. We selected two ROIs, including the RN and the presumed Vim, on axial images of the FGATIR sequence to construct a fiber tract that would pass through these two areas (Fig. 2). These two ROIs were selected on the axial slice at the level where the structure is most clearly shown. We set the FA threshold and minimum fiber length at 0.18 and 50 mm, respectively. If the tractography connecting two ROIs was successfully obtained, we considered that the selection of the ROIs was correct regardless of the successful delineation of the fibers connecting the RN with the contralateral dentate nucleus as the depiction of the crossing fibers is usually challenging for deterministic tractography methods [11,16–18]. However, when the tractography could not be delineated with the selected ROIs as anticipated, we checked the accuracy of our interpretation of the thalamic nuclei selected for an ROI prior to finalize the trajectory.

Typically, the trajectory is set at an approximate angle of 65 degrees with respect to the AC-PC line; however, in cases where it was difficult to determine a trajectory passing through the Vo/Vim border, it was instead passed through both the Vo and Vim, and was terminated in the posterior cZi at a 45–50 degree angle with respect to AC-PC line; this trajectory enabled the wide area in the thalamus to be stimulated, as reported by another investigation [19]. In cases with severe ventriculomegaly, the entry point is likely to be set laterally to avoid the lateral ventricle and the periventricular vein, so the target point is relatively medial to adjust the position of active electrodes in the thalamus and avoid the spread of the electrical current to the internal capsule. In either situation, we place a greater deal of weight on placing the active electrodes in the thalamus rather than the position of the electrode tip. Fig. 3 illustrates our method to optimize the trajectory angle.

2.3. Surgical procedure

The procedures of the present study were similar to those of our previous report [20]. On the morning of surgery, a Leksell G frame (Elekta, Sweden) was attached to the head after the injection of local anesthetics. A 5.5 cm straight skin incision was made. A burr hole, 14 mm in diameter, was fashioned and countersunk with a high-speed drill to prevent the burr hole cover (stimloc, Medtronic, Minneapolis) from protruding outside of the skull [15]. After we opened the dura, the pia was coagulated by bipolar cautery and sharply dissected using a #11 blade. Microelectrode recording (MER) was performed in select cases to map out the thalamic structures. Following implantation of a DBS electrode (model 3387, Medtronic, Minneapolis), macrostimulation was performed to test the threshold level of stimulation-induced side effects and the clinical efficacy; we ascertained that a minimum of 5 V were required for the intraoperative stimulation-induced side effects at all contacts to optimize the stimulation parameters at the clinical settings. The electrode was then fixed to the Burr hole cover. In cases where the safety margin of the DBS tract was low due to venous anatomy and/or large ventricular size, we did not perform MER; the DBS lead was implanted to the preoperatively presumed lead location.

An implantable pulse generator (IPG) was placed under general anesthesia, and electrical stimulation was started on the same day. Stimulation parameters were programmed at the clinical settings once a

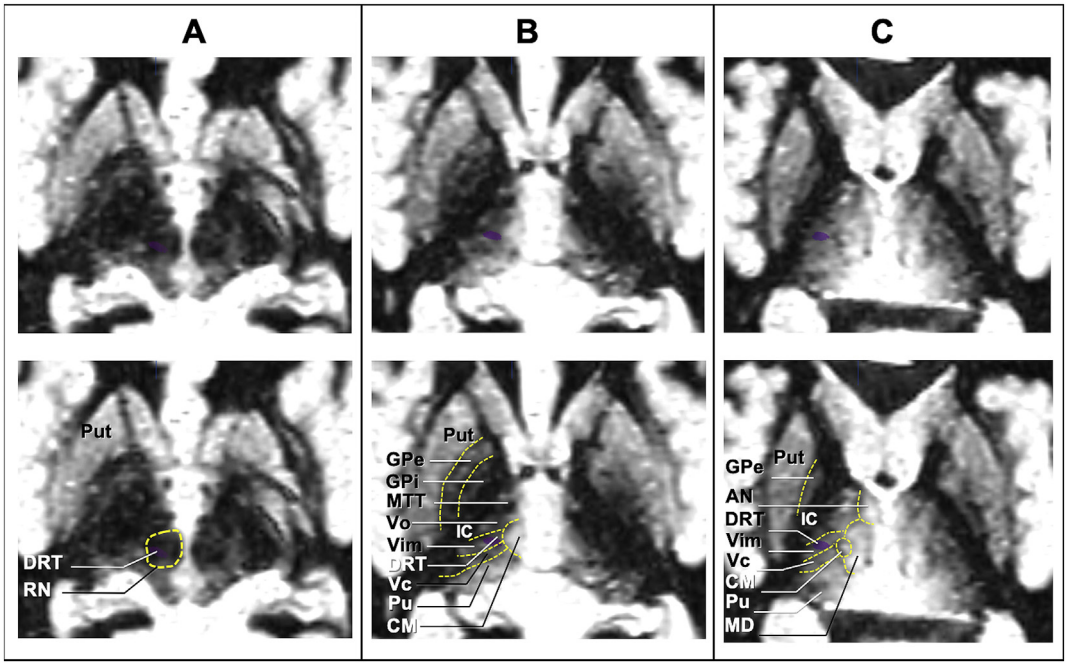

Fig. 1. Parcellation of thalamic nuclei on FGATIR axial images (Case 5). The images are organized ventral-to-dorsal in alphabetical order. The thalamic nuclei were classified by identifying the laminar in the thalamus (B-F, yellow dotted lines). The borders of the lenticular nuclei (B-E: yellow dotted lines) and the tractography of the dentate-rubro-thalamic tract are also depicted.
AN = Anterior Nucleus; CM = Centromedian nucleus; DRT = Dentate-Rubro-Thalamic Tract; GPe = Globus Pallidus externa; GPi = Globus Pallidus interna; IC = Internal Capsule; MTT = Mamillothalamic Tract; Put = Putamen; RN = Red Nucleus; Vc = Ventralis Caudalis nucleus; Vim = Ventral Intermediate nucleus; Vo = Ventralis Oralis. (For interpretation of the references to colour in this figure legend, the reader is referred to the web version of this article.)

month during the first 6 months, after which programming was performed as needed.

2.4. DBS lead localization

On postoperative day (POD) 10, when the pneumocephalus was fully resolved, a head CT scan was performed and fused to the preoperative MRI scan to measure the location of the DBS electrodes. Based on the same imaging studies, we also measured the location of the active contact for each case. These coordinates were measured relative to the MC point. We also retrospectively evaluated the positional relationship between the active contact and the depicted tract in each case.

3. Results

3.1. Clinical outcomes

During the study period, eight patients underwent unilateral thalamic DBS. All eight patients responded well to DBS therapy, but one patient with Parkinson's disease (PD) was excluded; he died of cholangiocarcinoma three months following surgery. We therefore analyzed the data from seven patients (3 men and 4 women); preoperative diagnoses included essential tremor (ET) (n = 3), PD (n = 2), and Holmes tremor (n = 2). Etiologies of Holmes tremor were stroke (n = 1) and severe head trauma (n = 1) (Fig. 4). The mean age and disease duration of our cohort were 70.0 ± 9.4 years and 4.1 ± 3.5 years, respectively. The mean follow-up periods were 11.1 ± 6.4 months. MER was not performed to minimize the number of electrode passes and operating time due to the medical concerns inclusive of liver cirrhosis (case 3), mild cognitive issue (case 3 and 5), and severe ex-vacuo change (Case 7). These demographics are summarized in Table 1.

All patients responded to DBS therapy; TRS motor scores improved from 28.1 ± 11.0 at baseline to 13 ± 7.4 (p = 0.018) and 13 ± 8.3 (p = 0.017) at the 6-month and last follow-up, respectively. TRS activities of daily living scores tended to improve from 13.3 ± 2.8 at baseline to 4.7 ± 7.2 (p = 0.063) and 5.5 ± 6.9 (p = 0.091) at the 6-month and last follow-up, respectively. Regarding the stimulation parameters, an interleaving stimulation setting configured with two contacts was used in three cases to stimulate wide areas of the thalamus; monopolar stimulation was administered in the remaining cases. Severe complications, such as intracranial hemorrhage and hardware infections, were not reported in our cohort. Clinical outcomes and the stimulation parameters are summarized in Table 2.

3.2. Parcellation of thalamic nuclei

Thalamic nuclei were consistently delineated on FGATIR images in our cohort as described in the methods section. Axial images provided the clearest depictions of the laminar separating thalamic nuclei. According to our anatomical interpretation of the FGATIR images, we were able to identify the following from anterior to posterior on the same axial plane: the mammillothalamic tract (MTT), Vo nucleus, Vim Nucleus, and Vc nucleus. The centromedian (CM) nucleus was located medially to the Vim nucleus. Median thalamic nuclei, such as the CM and mediodorsal (MD) nuclei, were observed as relatively high intensity areas on FGATIR images. In contrast, the MTT was depicted as a low intensity area; however, the termination in the anterior nucleus could still be identified. All thalamic structures could be clearly recognized. We could not, however, distinguish the Voa from the Vop, nor the CM from the parafascicullar (Pf) nuclei. The border between the Vc and pulvinar nuclei was less recognizable than the Vo/Vim and Vim/Vc borders.

3.3. Fiber tracking

The fiber tract passing through the presumed Vim thalamic nucleus

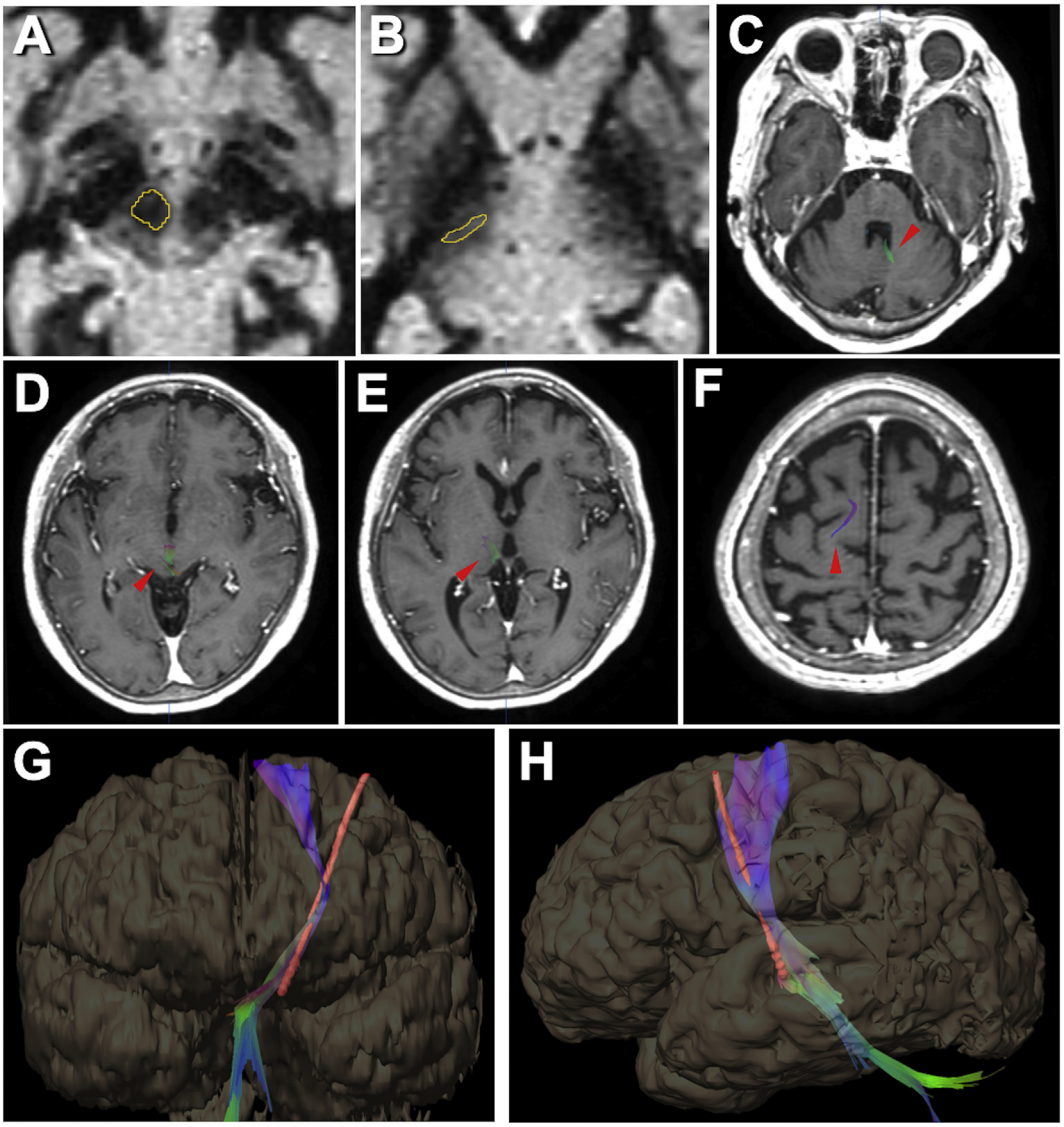

Fig. 2. Two regions of interest (A: red nucleus and B: ventral intermediate nucleus) depicted using a brush application within the software. The delineated dentate-rubro-thalamic tract on axial T1-weighted images at the level of dentete nucleus(C), red nucleus (D), thalamus (E), and precentral gyrus. 3D reconstruction images of the fiber tract and the DBS electrode (G and H). The images are obtained from case 1. (For interpretation of the references to colour in this figure legend, the reader is referred to the web version of this article.)

and the RN was consistently depicted in all cases prior to surgery. The obtained tract was considered to be the DRT, as the fiber terminated in the precentral gyrus. The obtained tracts also likely terminated in the medial area of the precentral gyrus in all cases. The present technique had some difficulty in delineating the fiber tracts crossing other fiber structures, such as the internal capsule or the superior cerebellar peduncle (Fig. 2). Four of seven cases had shown the cerebellorubral fibers passing through the decussation of superior cerebellar peduncle.

3.4. Stereotactic targeting coordinates and lead location

Three of the seven cases underwent MER mapping. The macrostimulation pass was not performed more than twice as the intraoperative threshold levels of the stimulation-induced side effect were acceptable in all cases. The mean coordinates of the stereotactic targeting were as follows: 11.1 ± 1.0 mm lateral, 5.4 ± 0.3 mm posterior, 2.0 mm inferior relative to the mid-commissural point. The trajectory angles were 28.4 ± 6.0 degrees relative to the midline plane (center-line angle) and 59.5 ± 9.1 degrees relative to the AC-PC plane (AC-PC angle). The mean coordinates of the tip of DBS electrode in our cohort were as follows: 10.9 ± 1.8 mm lateral, 6.0 ± 0.9 mm posterior, 1.7 ± 1.1 mm inferior relative to the mid-commissural point. The trajectory angles were 29.6 ± 4.8 degrees relative to the midline plane and 55.7 ± 10.3 relative to the AC-PC plane. These coordinates are summarized in Table 3.

All of the active contacts were located in the thalamus; however, four of ten active contacts were outside of the depicted fibers. The contacts located outside of the fibers were followings: contacts 1 and 3 in case 4, contact 2 in case 6, and contact 1 in case 7. The stimulation intensity of the contacts outside of the fiber tended to be higher. Especially, the stimulation intensity of case 4 was highest among cases even though the tremor was almost completely resolved. The relationship between the lead and the fiber is presented in Fig. 5 (Table 4).

4. Discussion

In this paper, we report seven tremor cases successfully treated with DBS. We acknowledge that FGATIR imaging has been employed in many experienced DBS centers; however, to the best of our knowledge,

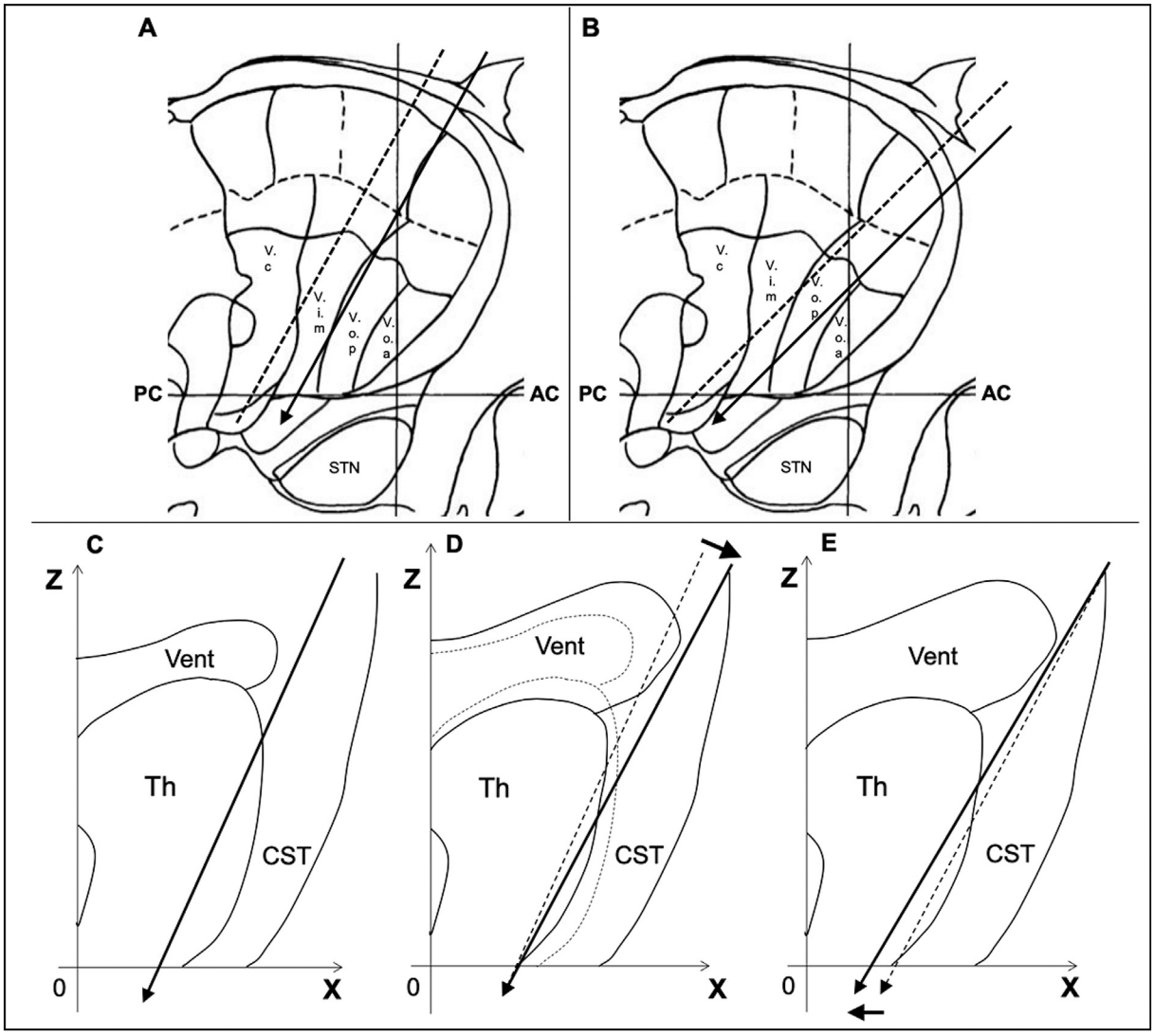

Fig. 3. A schema demonstrating different trajectories. (A) Typical DBS trajectory passing through the Vo/Vim border. (B) Low AC-PC angle passing through both Vo and Vim nuclei. Arrows and dotted lines indicate the trajectories of the DBS lead and microelectrode, respectively. It should be noted that the trajectory should be situated relatively posterior to pass through the wide areas of the thalamus when the lower AC-PC angle is selected. (C) The arrow indicates the DBS trajectory on coronal view in non-atrophic brain. (D) The trajectory angle relative to the midline becomes steep in a case with ventriculomegaly compared with that in non-atrophic brain. (E) In order to place the active contacts in the thalamus, the tip of the electrode is adjusted medially.
AC = anterior commissure; DBS = deep brain stimulation; CST = Cortico-spinal Tract; PC = posterior commissure; Vim = ventral intermediate; Vo = ventralis oralis; Th = Thalamus; Vent = Ventricle.

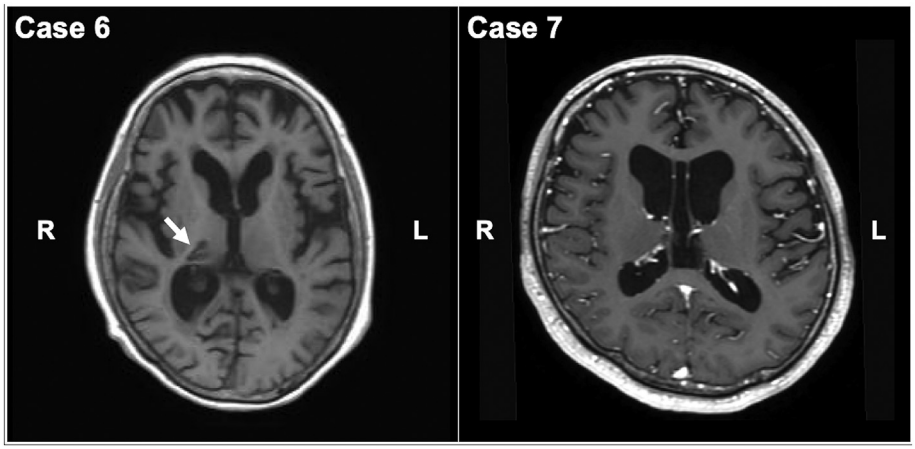

Fig. 4. MR images showing the stroke lesion (case 6) and the ventriculomegaly (case 7) in Holmes tremor cases.

Table 1
Patient demographics.

Case	Diagnosis	Age	Sex	Handedness	Disease duration (yrs)	DBS side	F/U (mo)
1	ET	65	F	Left	2	Left	24
2	ET	67	F	Right	4	Left	12
3	ET	80	M	Right	12	Left	12
4	PD, Tremor	72	F	Right	3	Left	12
5	PD, Tremor	73	M	Right	2	Left	6
6	Holmes Tremor	80	F	Right	3	Right	6
7	Holmes Tremor	51	M	Right	3	Left	6
		70.0 ± 9.4	3 men 4 women	Left 1 Right 6	4.1 ± 3.5	Left 6 Right 1	11.1 ± 6.4

F/U = Follow Up.

this is the first report describing the parcellation of the thalamic nuclei in combination with fiber tractography. Our results also suggest that the direct targeting of the thalamic target is feasible.

Recent publications have addressed the usefulness of fiber tractography in DBS surgery for the treatment of tremor [5,21]. However, the literature concerning the application of coordinate-based stereotactic targeting methods is inconsistent [4,7]; some have argued for direct targeting via fiber tractography. Clinicians should be aware that fiber tractography can be arbitrary, as the tract configuration can vary according to the methods [13]. The present report therefore used fiber tractography to support our anatomical interpretation of the thalamic nuclei on the FGATIR images rather than completely depending on the tractography.

Even though the depicted DRT was acceptable for stereotactic planning in all cases, the tractography images were not perfectly accurate as we used a commercialized planning software applying the deterministic fiber tractography methods that has weakness in delineating the crossing fibers [16,18]. To address the issue, probabilistic tractography methods may be useful to accurately delineate the DRT [11] or interpret the parcellation of the thalamic nuclei as demonstrated by recent studies [22–24]. Interestingly, Middlebrooks and colleagues reported the greater volume of activation (VTA) in the motor-related area in the thalamus was associated with favorable outcomes [24]. However, it should be noted that the probabilistic tractography has been research-based while our methods are useful even in busy clinical settings.

We have focused on the stimulation of the thalamic nuclei, but there have been arguments concerning the optimal target for electrical stimulation [25–27]. Blomstedt and colleagues have reported the favorable outcomes of the posterior subthalamic area (PSA) stimulation for essential tremor [24,25]. According to their studies, the PSA stimulation was more effective and required lower stimulation intensity than other targets such as Vim and subthalamic nucleus (STN) [25,26]. Based on these findings, it may be desirable to implant the DBS electrode passing through the Vim thalamic nucleus to the subthalamic area as proposed by another group [8]. However, the insertion angle is usually determined by the individual anatomy for safety so the trajectory with lower angles relative to the AC-PC plane to stimulate the wide area of in the thalamus may be an option as shown in our case. On the other hand, as a recent study showed the efficacy of the globus pallidus interna (GPi) stimulation for Holmes tremor cases [28], the optimal target may be selected according to the etiology.

It should be noted that tremor was successfully controlled even in Holmes tremor cases, for which DBS has been considered less effective than when performed for the treatment of other tremor disorders. To address Holmes tremor, a large thalamotomy lesion was reportedly required [29], and several other studies have imitated the large lesion by implanting two leads in the thalamus [8,15,30,31]. Our results showed that the DBS was likely to stimulate the wide range of the thalamus at a relatively high voltage; this was achieved by implanting the DBS lead medially at a lower AC-PC angle as proposed by Yamamoto et al. [19]. We consider that the accurate placement of the DBS lead is important to address tremor regardless of its etiology. We suspect that unsuccessful outcomes in the treatment of Holmes tremor may be partly due to suboptimal placement of the DBS lead, as the ex-vacuo change in Holmes tremor cases renders the preoperative stereotactic targeting more complicated.

Although our method has demonstrated potential, it features several important limitations. The present study was an open label, non-controlled study that included a limited number of heterogeneous tremor cases with three different etiologies. Controlled studies with a greater number of patients should therefore be conducted to confirm our findings. Further, we interpreted anatomy delineated on MR images based on a human brain. Even though the clinical outcomes supported our anatomical interpretation, our findings should be confirmed by other imaging modalities with quantitative analysis, such as MRI with a higher magnetic field (e.g., 7 T MRI), probabilistic tractography, and/or electrical field model.

5. Conclusion

We demonstrated a new method to identify the DBS trajectory using

Table 2
Clinical outcomes and the stimulation parameters at last follow-up.

No.	TRS motor score			TRS ADL score		
	Baseline	6mo	Last F/U	Baseline	6mo	Last F/U
1	29	12	16	15	2	3
2	31	13	13	14	4	6
3	24	16	18	9	2	4
4	14	2	1	11	1	1
5	48	24	24	15	19	19
6	32	18	18	12	18	18
7	19	6	6	17	0	0
Mean ± SD	28.1 ± 11.0	13 ± 7.4[a]	13 ± 8.3[a]	13.3 ± 2.8	4.7 ± 7.2	5.5 ± 6.9

TRS = Tremor Rating Scale.
[a] Statistically significant improvement.

Table 3
Preoperative stereotactic targeting coordinates and the postoperative lead tip location.

No.	MER	Preop stereotactic targeting coordinate					Postop lead tip location				
		Lat	AP	AX	Ctr-Line Angle	AC-PC Angle	Lat	AP	AX	Ctr-Line Angle	AC-PC Angle
1	+	11.5	−5.5	−2	25.7	68.7	10.7	−4.9	−2.5	25.8	66.7
2	−	10	−5.5	−2	26.6	56	11.2	−6.0	−1.65	25.3	51.3
3	−	12.5	−5.5	−2	26.1	65.3	12.5	−5.5	−2	26.1	65.3
4	+	9.5	−6.0	−2	28.1	47.2	9.0	−6.6	−0.24	30.7	43.5
5	−	10.5	−5.5	−2	27.5	68	8.8	−6.6	−2.52	28.7	66.4
6	+	11	−5.0	−2	30	51	10.3	−4.6	−3.05	31.7	52.0
7	−	12	−5	−2	42	51	14.2	−7.0	−1.81	39.0	44.5
		11.1 ± 1.0	−5.4 ± 0.3	−2.0 ± 0.0	28.4 ± 6.0	59.5 ± 9.1	10.9 ± 1.8	−6.0 ± 0.9	−1.7 ± 1.1	29.6 ± 4.8	55.7 ± 10.3

AC = Anterior Commissure; Ctr = Center; MER = Microelectrode Recording; PC = Posterior Commissure; 3 V = Third Ventricle.

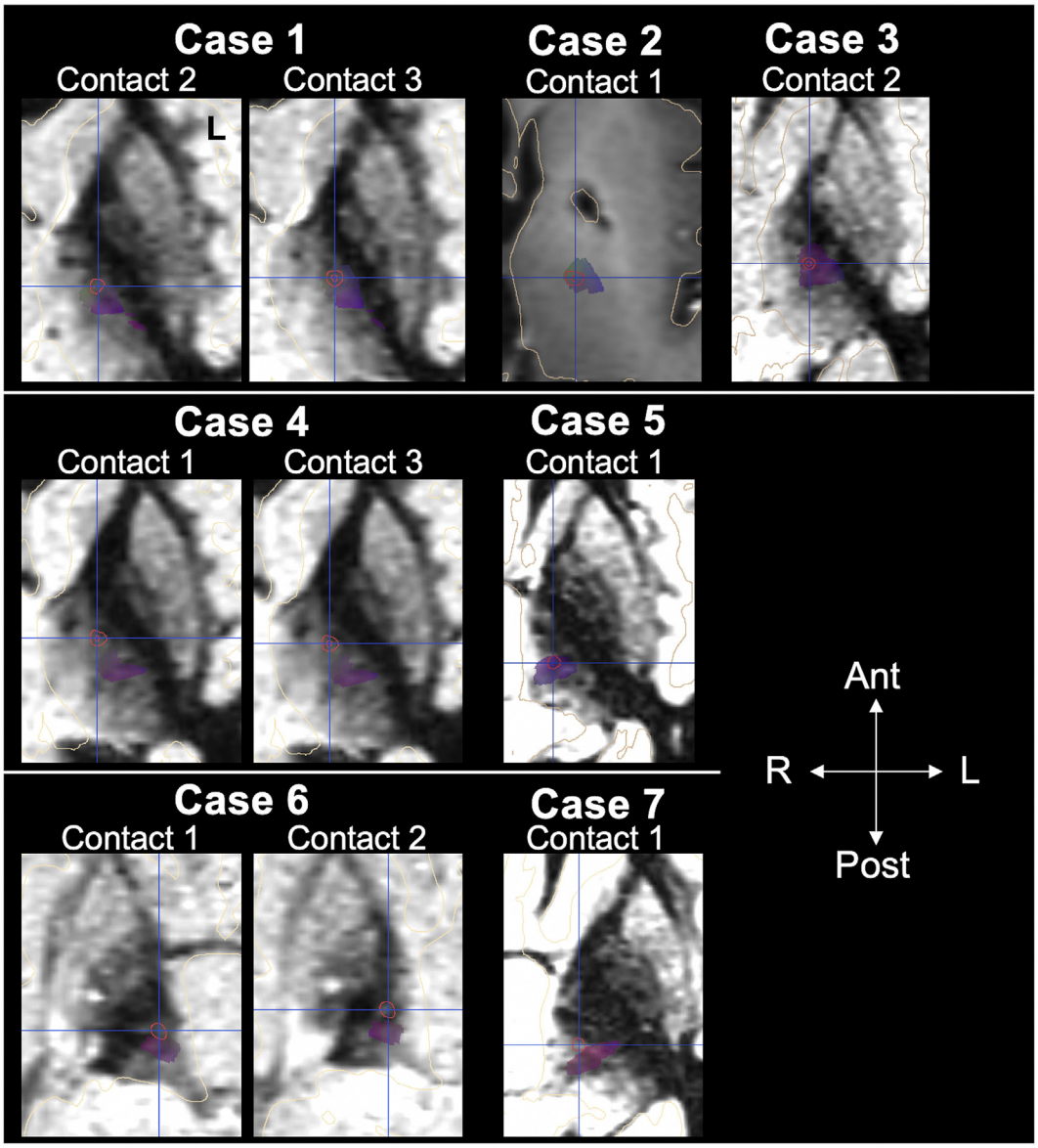

Fig. 5. The location of the active contacts relative to the preoperatively depicted fiber tractography on axial images. All images are FGATIR sequence except for case 2 showing T1-weighted image due to lack of sufficient quality FGATIR image. Crosshairs indicates the center of the active contact (red circle), and flesh colour lines indicate the contour of the ventricles and gyrus. Four of ten active contacts located outside of the fibers were following: contacts 1 and 3 in case 4, contact 2 in case 6, and contact 1 in case 7. (For interpretation of the references to colour in this figure legend, the reader is referred to the web version of this article.)

Table 4
The stimulation parameters and the position of the active contacts at last follow-up.

No.	Stimulation parameters at last visit					Coordinates of active contacts		
	Cathode	Anode	PW (μsec)	Frequency (Hz)	Voltage (v)	X	Y	Z
1[a]	2	Case	90	125	3.0	13.3	−2.0	3.3
	3	Case	90	125	3.5	14.5	−1.0	5.9
2	1	3	120	180	2.6	13.5	−2.0	3.7
3	2	Case	120	200	3.4	16.6	−2.8	3.3
4[a]	1[b]	Case	120	120	3.4	10.4	−3.7	1.9
	3[b]	Case	210	120	4.4	12.6	0.4	5.9
5	1	Case	60	130	3.0	11.0	−5.2	0.9
6[a]	1	Case	120	125	2.8	12.2	−2.0	0.6
	2[b]	Case	120	125	3.2	13.7	−0.4	2.5
7	1[b]	Case	60	150	3.2	16.3	−4.6	0.3

TRS = Tremor Rating Scale.
[a] Interleaving stimulation settings were applied.
[b] These active contacts were outside of the fiber tract as shown in Fig. 5.

high-resolution MRI images and supplemental fiber tractography. As demonstrated by the fiber tractography and clinical outcomes, the Vim nucleus may be determined using the FGATIR sequence. Our methods are feasible and effective in accurately identifying the optimal DBS trajectory. We advocate that surgeons performing DBS procedures should interpret the anatomical information from preoperative imaging studies for accurate DBS implantation in each case, rather than perform a coordinate-based surgery. In this context, the anatomic descriptions provided by our paper may be useful in improving DBS techniques.

Funding

This study was partly supported by Japan Society for the Promotion of Science (JSPS) Grant-in-Aid for Scientific Research (C)18K08956, JSPS Fujita Memorial Fund for Medical Research and Takeda Science Foundation.

Declarations of interest

None.

References

[1] V.A. Coenen, N. Allert, B. Madler, A role of diffusion tensor imaging fiber tracking in deep brain stimulation surgery: DBS of the dentato-rubro-thalamic tract (drt) for the treatment of therapy-refractory tremor, Acta Neurochir. 153 (8) (2011) 1579–1585 (discussion 1585).
[2] V.A. Coenen, B. Madler, H. Schiffbauer, H. Urbach, N. Allert, Individual fiber anatomy of the subthalamic region revealed with diffusion tensor imaging: a concept to identify the deep brain stimulation target for tremor suppression, Neurosurgery 68 (4) (2011) 1069–1075 (discussion 1075-6).
[3] V.A. Coenen, M. Rijntjes, T. Prokop, T. Piroth, F. Amtage, H. Urbach, P.C. Reinacher, One-pass deep brain stimulation of dentato-rubro-thalamic tract and subthalamic nucleus for tremor-dominant or equivalent type Parkinson's disease, Acta Neurochir. 158 (4) (2016) 773–781.
[4] A.J. Fenoy, M.C. Schiess, Deep Brain Stimulation of the Dentato-Rubro-Thalamic Tract: Outcomes of Direct Targeting for Tremor, Neuromodulation 20 (5) (2017) 429–436.
[5] J.M. Henderson, "Connectomic surgery": diffusion tensor imaging (DTI) tractography as a targeting modality for surgical modulation of neural networks, Front. Integr. Neurosci. 6 (2012) 15.
[6] T. Chen, Z. Mirzadeh, K. Chapple, M. Lambert, R. Dhall, F.A. Ponce, "Asleep" deep brain stimulation for essential tremor, J. Neurosurg. 124 (6) (2016) 1842–1849.
[7] K.A. Nestor, J.D. Jones, C.R. Butson, T. Morishita, C.E.t. Jacobson, D.A. Peace, D. Chen, K.D. Foote, M.S. Okun, Coordinate-based lead location does not predict Parkinson's disease deep brain stimulation outcome, PLoS ONE 9 (4) (2014) e93524.
[8] S.F. Oliveria, R.L. Rodriguez, D. Bowers, D. Kantor, J.D. Hilliard, E.H. Monari, B.M. Scott, M.S. Okun, K.D. Foote, Safety and efficacy of dual-lead thalamic deep brain stimulation for patients with treatment-refractory multiple sclerosis tremor: a single-Centre, randomised, single-blind, pilot trial, Lancet Neurol. 16 (9) (2017) 691–700.
[9] A. Sudhyadhom, I.U. Haq, K.D. Foote, M.S. Okun, F.J. Bova, A high resolution and high contrast MRI for differentiation of subcortical structures for DBS targeting: the fast gray matter acquisition T1 inversion recovery (FGATIR), NeuroImage 47 (Supplement 2) (2009) T44–T52.
[10] M.N. Gallay, D. Jeanmonod, J. Liu, A. Morel, Human pallidothalamic and cerebellothalamic tracts: anatomical basis for functional stereotactic neurosurgery, Brain Struct. Funct. 212 (6) (2008) 443–463.
[11] H.G. Kwon, J.H. Hong, C.P. Hong, D.H. Lee, S.H. Ahn, S.H. Jang, Dentatorubrothalamic tract in human brain: diffusion tensor tractography study, Neuroradiology 53 (10) (2011) 787–791.
[12] K. Yamada, K. Akazawa, S. Yuen, M. Goto, S. Matsushima, A. Takahata, M. Nakagawa, K. Mineura, T. Nishimura, MR imaging of ventral thalamic nuclei, AJNR Am. J. Neuroradiol. 31 (4) (2010) 732–735.
[13] A. Nowacki, J. Schlaier, I. Debove, C. Pollo, Validation of diffusion tensor imaging tractography to visualize the dentatorubrothalamic tract for surgical planning, J. Neurosurg. (2018) 1–10.
[14] G. Schaltenbrand, W. Wahren, Atlas for Stereotaxy of the Human Brain, Year Book Medical Publishers, Chicago, 1977.
[15] K.D. Foote, M.S. Okun, Ventralis intermedius plus ventralis oralis anterior and posterior deep brain stimulation for posttraumatic Holmes tremor: two leads may be better than one: technical note, Neurosurgery 56 (2 Suppl) (2005) (E445; discussion E445).
[16] K. Yamada, K. Sakai, K. Akazawa, S. Yuen, T. Nishimura, MR tractography: a review of its clinical applications, Magn. Reson. Med. Sci. 8 (4) (2009) 165–174.
[17] G.J. Parker, D.C. Alexander, Probabilistic anatomical connectivity derived from the microscopic persistent angular structure of cerebral tissue, Philos. Trans. R. Soc. Lond. Ser. B Biol. Sci. 360 (1457) (2005) 893–902.
[18] V.A. Coenen, B. Varkuti, Y. Parpaley, S. Skodda, T. Prokop, H. Urbach, M. Li, P.C. Reinacher, Postoperative neuroimaging analysis of DRT deep brain stimulation revision surgery for complicated essential tremor, Acta Neurochir. 159 (5) (2017) 779–787.
[19] T. Yamamoto, Y. Katayama, T. Kano, K. Kobayashi, H. Oshima, C. Fukaya, Deep brain stimulation for the treatment of parkinsonian, essential, and poststroke tremor: a suitable stimulation method and changes in effective stimulation intensity, J. Neurosurg. 101 (2) (2004) 201–209.
[20] T. Morishita, M.A. Higuchi, K. Saita, Y. Tsuboi, H. Abe, T. Inoue, Changes in motor-related cortical activity following deep brain stimulation for Parkinson's Disease detected by functional near Infrared Spectroscopy: a pilot study, Front. Hum. Neurosci. 10 (2016) 629.
[21] E. Calabrese, Diffusion tractography in deep brain stimulation surgery: a review, Front. Neuroanat. 10 (2016) 45.
[22] E.H. Middlebrooks, I.S. Tuna, S.S. Grewal, L. Almeida, M.G. Heckman, E.R. Lesser, K.D. Foote, M.S. Okun, V.M. Holanda, Segmentation of the globus pallidus internus using probabilistic diffusion tractography for deep brain stimulation targeting in Parkinson disease, AJNR Am. J. Neuroradiol. 39 (6) (2018) 1127–1134.
[23] E.H. Middlebrooks, V.M. Holanda, I.S. Tuna, H.D. Deshpande, M. Bredel, L. Almeida, H.C. Walker, B.L. Guthrie, K.D. Foote, M.S. Okun, A method for preoperative single-subject thalamic segmentation based on probabilistic tractography for essential tremor deep brain stimulation, Neuroradiology 60 (3) (2018) 303–309.
[24] E.H. Middlebrooks, I.S. Tuna, L. Almeida, S.S. Grewal, J. Wong, M.G. Heckman, E.R. Lesser, M. Bredel, K.D. Foote, M.S. Okun, V.M. Holanda, Structural connectivity-based segmentation of the thalamus and prediction of tremor improvement following thalamic deep brain stimulation of the ventral intermediate nucleus, Neuroimage Clin. 20 (2018) 1266–1273.
[25] U. Sandvik, L.O. Koskinen, A. Lundquist, P. Blomstedt, Thalamic and subthalamic deep brain stimulation for essential tremor: where is the optimal target? Neurosurgery 70 (4) (2012) 840–845 (discussion 845-6).
[26] P. Blomstedt, U. Sandvik, J. Linder, A. Fredricks, L. Forsgren, M.I. Hariz, Deep brain stimulation of the subthalamic nucleus versus the zona incerta in the treatment of essential tremor, Acta Neurochir. 153 (12) (2011) 2329–2335.
[27] T. Morishita, Y. Tsuboi, M.A. Higuchi, T. Inoue, Letter to the Editor: is one large target better than two? J. Neurosurg. 123 (5) (2015) 1349.
[28] C. Kilbane, A. Ramirez-Zamora, E. Ryapolova-Webb, S. Qasim, G.A. Glass, P.A. Starr, J.L. Ostrem, Pallidal stimulation for Holmes tremor: clinical outcomes

and single-unit recordings in 4 cases, J. Neurosurg. (2015) 1–9.
[29] T. Hirai, M. Miyazaki, H. Nakajima, T. Shibazaki, C. Ohye, The correlation between tremor characteristics and the predicted volume of effective lesions in stereotaxic nucleus ventralis intermedius thalamotomy, Brain 106 (Pt 4) (1983) 1001–1018.
[30] K.D. Foote, P. Seignourel, H.H. Fernandez, J. Romrell, E. Whidden, C. Jacobson, R.L. Rodriguez, M.S. Okun, Dual electrode thalamic deep brain stimulation for the treatment of posttraumatic and multiple sclerosis tremor, Neurosurgery 58 (4 Suppl 2) (2006) (ONS-280-5; discussion ONS-285-6).
[31] T. Yamamoto, Y. Katayama, C. Fukaya, H. Oshima, M. Kasai, K. Kobayashi, New method of deep brain stimulation therapy with two electrodes implanted in parallel and side by side, J. Neurosurg. 95 (6) (2001) 1075–1078.